J Periodontal Implant Sci. 2022 Apr;52(2):155-169
https://doi.org/10.5051/jpis.2101200060
pISSN 2093-2278·eISSN 2093-2286

JPIS
Journal of Periodontal & Implant Science

Research Article
Implant Science

Check for updates

Insulin growth factor binding protein-3 enhances dental implant osseointegration against methylglyoxal-induced bone deterioration in a rat model

Jyoti Shrestha Takanche [1,2,†], **Ji-Eun Kim** [1,†], **Sungil Jang** [1], **Ho-Keun Yi** [1,*]

[1]Department of Oral Biochemistry, Institute of Oral Bioscience, School of Dentistry, Jeonbuk National University, Jeonju, Korea
[2]Department of Biochemistry, School of Medical Sciences, Kathmandu University, Nepal

OPEN ACCESS

Received: Feb 9, 2021
Revised: Jul 8, 2021
Accepted: Jul 9, 2021
Published online: Sep 23, 2021

***Correspondence:**
Ho-Keun Yi
Department of Oral Biochemistry, School of Dentistry, Jeonbuk National University, 567 Baekje-daero, Deokjin-gu, Jeonju 54896, Korea.
Email: yihokn@chonbuk.ac.kr
Tel: +82-63-270-4033

[†]Jyoti Shrestha Takanche and Ji-Eun Kim contributed equally to the work.

ORCID iDs
Jyoti Shrestha Takanche
https://orcid.org/0000-0003-2375-190X
Ji-Eun Kim
https://orcid.org/0000-0003-4683-4775
Sungil Jang
https://orcid.org/0000-0001-6144-6899
Ho-Keun Yi
https://orcid.org/0000-0003-4403-3827

Funding
This work was supported by a grant from the National Research Foundation (NRF) of Korea, funded by the Korean government (MSIP) [(NRF-2018R1A2B6004744).

ABSTRACT

Purpose: The aim of this study was to determine the effect of insulin growth factor binding protein-3 (IGFBP-3) on the inhibition of glucose oxidative stress and promotion of bone formation near the implant site in a rat model of methylglyoxal (MGO)-induced bone loss.
Methods: An *in vitro* study was performed in MC3T3 E1 cells treated with chitosan gold nanoparticles (Ch-GNPs) conjugated with *IGFBP-3* cDNA followed by MGO. An *in vivo* study was conducted in a rat model induced by MGO administration after the insertion of a dental implant coated with *IGFBP-3*.
Results: MGO treatment downregulated molecules involved in osteogenic differentiation and bone formation in MC3T3 E1 cells and influenced the bone mineral density and bone volume of the femur and alveolar bone. In contrast, IGFBP-3 inhibited oxidative stress and inflammation and enhanced osteogenesis in MGO-treated MC3T3 E1 cells. In addition, IGFBP-3 promoted bone formation by reducing inflammatory proteins in MGO-administered rats. The application of Ch-GNPs conjugated with *IGFBP-3* as a coating of titanium implants enhanced osteogenesis and the osseointegration of dental implants.
Conclusions: This study demonstrated that IGFBP-3 could be applied as a therapeutic component in dental implants to promote the osseointegration of dental implants in patients with diabetes, which affects MGO levels.

Keywords: Antioxidants; Bone formation; Diabetes mellitus; Inflammation; MC3T3 E1

INTRODUCTION

Diabetes mellitus (DM) is a systemic disease that is the most prevalent chronic condition worldwide [1]. DM is associated with complications caused by micro- and macro-angiopathies, which increase the frequency of impaired responses to infections, delayed wound healing, periodontitis, tooth loss, and the risk of fracture [2,3]. Similarly, DM is associated with impaired bone density, mineralization, and turnover [4]. Many clinical studies have demonstrated that DM has an unfavorable impact on implant osseointegration

The μCT samples were analyzed using a model 1076 apparatus (Skyscan, Kontich, Belgium) installed in the Center for University-Wide Research Facilities (CURF) at Jeonbuk National University.

Author Contributions

Conceptualization: Jyoti Shrestha Takanche, Ji-Eun Kim, Ho-Keun Yi; Formal aalysis: Ji-Eun Kim, Sungil Jang, Ho-Keun Yi; Investigation: Jyoti Shrestha Takanche, Ho-Keun Yi; Methodology: Jyoti Shrestha Takanche, Ji-Eun Kim; Project administration: Ji-Eun Kim, Sungil Jang, Ho-Keun Yi; Writing - original draft: Jyoti Shrestha Takanche, Ji-Eun Kim; Writing - review & editing: Ho-Keun Yi.

Conflict of Interest

No potential conflict of interest relevant to this article was reported.

and stability, eventually leading to implant failure [5,6]. Consequently, implant therapy remains a relative contraindication in DM patients unless the disease is well-controlled [7,8].

Methylglyoxal (MGO) is a highly reactive dicarbonyl compound generated as an intermediate of glycolysis that is considered a potent precursor of advanced glycation end products (AGEs) [9,10]. The process of AGE generation from MGO is also associated with the formation of reactive oxygen species (ROS) [11]. Many research studies have suggested that DM may lead to impairments of cognitive processes through a mechanism that includes both AGE formation and oxidative stress [12,13]. Accordingly, high levels of MGO may cause DM-related cognitive degeneration, and MGO toxicity may be responsible for DM-associated bone loss [14]. Previous studies have demonstrated that MGO treatment can be a risk factor for bone loss by inducing apoptosis in human osteoblasts [15]. In addition, MGO causes loss of bone mineral density in experimental animal models [16]. MGO was found to contribute to the delayed healing of bone in a diabetic rat model, and it has been suggested that detoxification of MGO is important for improving bone repair in patients with diabetes [17].

Titanium (Ti) dental implants are widely used for the replacement of extracted or missing teeth [18]. In patients with poor bone quality, various techniques, including surface chemistry, implant design, and surface topography, have been applied for the improvement of dental implant osseointegration [19]. Implant surface modification using a gene delivery system is a technique used for bone regeneration near implants [20]. Nanoparticles are considered the best carriers for desirable genes to the targeted area due to their transfection efficiency [21]. The delivery of genes with bioactive characteristics of biocompatibility and bone regeneration through dental implants has been highly recommended [22,23]. In a previous study, chitosan gold nanoparticles (Ch-GNPs) conjugated with *PPARγ* cDNA were introduced on Ti implant surfaces for *PPARγ* release in the rat mandible [24].

Bone healing can be improved by various growth factors, such as platelet-derived growth factor, bone morphogenetic proteins (BMPs), transforming growth factor β isoforms, and insulin-like growth factors (IGFs) [25]. Among the IGF binding protein (IGFBP) family, IGFBP-3, which binds circulating IGF-I/II, is the most abundant IGFBP in bone tissue [26,27]. Some studies have suggested that IGFBP-3 plays a positive role in bone formation by binding with type I collagen and that IGFs are stored in the skeletal matrix [28]. IGFBP-3 also acts on the growth plate and supports bone formation [29]. Some evidence suggests that IGFBP-3 promotes human tooth development in the late stages [30]. IGFBP-3 is also involved in the tumor suppressor functions of cancer cells [31,32].

Our previous study also demonstrated the delivery of the *IGFBP-3* gene by Ch-GNPs and the potential role of IGFBP-3 in bone formation in the rat mandible [27]. However, the role of *IGFBP-3* in bone deterioration due to MGO has not been elucidated. Considering the benefits of *IGFBP-3* gene delivery for bone formation, this study demonstrated the anti-inflammatory effects of IGFBP-3 in MGO-induced cells and explored the osseointegration and bone improvement in response to Ch-GNP/*IGFBP-3*-coated Ti implants in an MGO-induced rat model.

https://doi.org/10.5051/jpis.2101200060

MATERIALS AND METHODS

MC3T3 E1 cell culture and MGO treatment

MC3T3 E1 cells (DCRL-2593; American Tissue Type Collection, Manassas, VA, USA) were cultured in α-MEM (Gibco BRL, Grand Island, NY, USA) supplemented with 2 mM glutamine, 100 U/mL penicillin, 100 μg/mL streptomycin, and 10% fetal bovine serum in a humidified 5% CO_2 atmosphere at 37°C and sub-cultured at a 1:4 ratio. The mineralization experiments for Alizarin red staining and alkaline phosphatase (ALP) activity were performed with MC3T3 E1 cells cultured in 50 μg/mL ascorbic acid, 10 mM β-glycerophosphate, and 100 nM dexamethasone, as previously described [33]. To confirm the response of MGO-treated MC3T3 E1 cells, 80% confluent cells were exposed to MGO (400 μM); fresh medium was replaced 2 hours later, and the cells were cultured for 15 days.

Preparation of Ch-GNPs

Ch-GNPs were prepared by a simple graft-on technique as previously described [27]. Briefly, 2 mL of 0.33% chitosan solution and 0.1 M hydrochloric acid (HCl) was mixed with 1 mL of a 10 mM freshly prepared chloroauric acid ($HAuCl_4$) solution and stirred for 1 hour. Later, the prepared solution was constantly mixed with 0.1 M ice-cold, freshly prepared sodium borohydrate. A rapid change to a red wine color indicated the formation of Ch-GNPs. The Ch-GNPs were collected by ultracentrifugation at 35,000 × *g* at 4°C for 30 minutes. The Ch-GNP stock solution was used in triple-distilled water for further experimentation.

Preparation of DNA complexes

Complexes of Ch-GNPs and plasmid DNA (pcDNA3.1 *IGFBP-3* and *LacZ*) were prepared as previously described [23]. In brief, the Ch-GNPs and plasmid DNA (pcDNA3.1 *IGFBP-3*, pcDNA3.1 *LacZ*, Invitrogen, Carlsbad, CA, USA) were used to prepare the complexes in water, and the Ch-GNP solution (40 μg) from the stock solution (50 mg/mL) of nanoparticles was mixed with 20 μg of DNA.

Loading of Ch-GNP/DNA complexes on Ti surfaces and mini-screws

The cDNA of *LacZ* and *IGFBP-3* was cloned in plasmid DNA. The Ch-GNP/DNA complexes were deposited on cleaned Ti surfaces (6×6×0.1 cm for a 100-mm cell dish), using the dipping technique at room temperature. The Ch-GNP/DNA solution was mixed with 500 μL of serum and antibiotic-free medium, and the surface was coated with it, followed by drying at room temperature. The Ti surface coated with Ch-GNPs/*IGFBP-3* was placed in a 100-mm-diameter cell culture plate, the same number of cells (5×10^5) were seeded on the plate, and 1 mL of cell culture medium was added. After 3 hours, the cell culture medium was replaced with a fresh medium. For *in vivo* analysis, dental implants were prepared as previously described [22]. Briefly, commercially available pure, cylindrically shaped Ti square thread screws (4.5 mm in length and 0.85 mm in diameter) were used as dental implants. For coating with Ch-GNPs/*IGFBP-3* and *LacZ*, the implants were immersed 10 times in a nanoparticle DNA solution and frozen at −40°C. The total coating amount of the DNA was 20 μg each. Ch-GNP/*LacZ*-coated implants were used as a control.

Western blot analysis

A previously described method was used for western blot analysis [27]. In brief, total proteins were extracted from the MC3T3 E1 cells with a lysis buffer containing 150 mM NaCl, 5 mM EDTA, 50 mM Tri-HCl (pH 8.0), 1% NP 40, 1 mM pepstatin, 1 mM aprotinin, and 0.1 mM leupeptin. Proteins in the cells were quantified by the Bradford dye-binding procedure

https://doi.org/10.5051/jpis.2101200060

(Bio-Rad, Hercules, CA, USA). The samples were separated by sodium dodecyl sulfate-polyacrylamide gel electrophoresis (8% to 15%) under denaturing conditions and transferred to a Hybond-P membrane (Amersham, Arlington, IL, USA). Specific primary antibodies were used at a ratio of 1:1,000 to 1:2,000 and incubated at 4°C overnight, and then incubated with a horseradish peroxidase-IgG-conjugated secondary antibody at room temperature for 1 hour. A chemiluminescence detection reagent was used to detect the signals according to the manufacturer's protocol (Amersham Pharmacia Biotech, London, UK) with a LAS-4000 CCD imaging system (Fujifilm, Tokyo, Japan).

Alizarin red staining and ALP activity

Alizarin red staining was performed in the MC3T3 E1 cells after 3, 6, 9, 12, and 15 days of differentiation induction culture. After the indicated times of cell culture, the cells were washed with phosphate-buffered saline (PBS), air-dried, and fixed in 95% ice-cold ethanol at −20°C for 30 minutes. After fixation, the cells were stained with 40 mM of Alizarin red stain (pH 4.2) at room temperature for 1 hour. The plates were washed with deionized water 5 times and then rinsed with PBS (without magnesium and calcium) for 15 minutes.

ALP activity was measured in MC3T3 E1 cells collected in cold PBS at 3, 6, 9, 12, and 15 days and sonicated with a cell disruptor (Heat System-Ultrasonics, Plainview, NJ, USA) in an ice bath. ALP activity in the supernatant was measured using the SensoLyte pNPP Alkaline Phosphatase Assay Kit (AnaSpec, Inc., Fremont, CA, USA) according to the manufacturer's protocol [34].

Determination of ROS generation

ROS generation of MC3T3 E1 cells was measured by the Muse Oxidative stress kit using the Muse cell analyzer (Merck Millipore, KGaA, Darmstadt, Germany) as a fluorescent-based analytical technique. The manufacturer-specific protocol was followed for the assay. In brief, MC3T3 E1 cells were treated with *LacZ* and *IGFBP-3* for 1 hour prior to MGO (400 μM) treatment and incubated for 24 or 48 hours. Samples of 1×10^7 cells/mL were prepared in 1× assay buffer and treated with an oxidative stress reagent based on dihydroethidium; this reagent is used to detect ROS that are oxidized with superoxide anion to produce the DNA-binding fluorophore ethidium bromide, which intercalates with DNA, resulting in red fluorescence.

Animals and surgical procedures

The Animal Ethical Committee of Jeonbuk National University (CBNU-2019-00299) approved the protocol for the use of animals in the study. Six-week-old Sprague-Dawley male rats were used in the experiment. The animals were randomly assigned to 4 groups: no MGO administration (control; n = 12), MGO administration (MGO; n = 12), MGO administration with Ch-GNPs/*LacZ* (MGO-*LacZ*; n = 12), and MGO administration with Ch-GNPs/*IGFBP-3* (MGO-*IGFBP-3*; n = 12). The dosage of MGO was determined according to previous studies [35]. First, to observe changes in bone quality by MGO *in vivo*, PBS was injected into the control group and 75 mg/kg of MGO was injected into the MGO group twice a week for a total of 6 weeks. All surgical procedures were performed under general anesthesia induced with zolazepam (Zoletil 50; Virbac Carros, France) and xylazine hydrochloride (Rompun; Bayer Korea, Seoul, Korea). The lower first molar was extracted carefully to avoid damage to the extraction socket. The animals were given intramuscular injections of amikacin for up to 3 days. At 1 week after tooth extraction, 75 mg/kg of MGO was intraperitoneally injected into both groups twice a week for a total of 10 weeks. At 4 weeks after tooth extraction, the specified implants were inserted into the indicated groups. After 3 and 6 weeks, the rats were euthanized by cervical dislocation under general anesthesia, and samples were collected for examination.

https://doi.org/10.5051/jpis.2101200060

Micro-computed tomography analysis

Micro-computed tomography (μCT) was performed with an anode electrical current of 100 kV at a resolution of 18 μm using a model 1076 apparatus (Skyscan, Kontich, Belgium). After anesthesia, the femur and mandibles were scanned with μCT to detect dynamic changes in the tissues and peri-implant tissue at 3 and 6 weeks. The regions of interest (ROIs) that included the trabecular compartment around the femur were selected. The ROI of the alveolar bone was manually established in the interradicular septum bone of the right mandibular first molar (M1) without an implant. The coronal and horizontal planes of M1 were confirmed by 2-dimensional images, which were generated by DataViewer (Skyscan). First, in the coronal plane passing through the center of the buccal and lingual roots, 2 horizontal surfaces were selected that individually passed through the alveolar ridge crest and apex of the buccal root. Second, on the horizontal plane of the M1 tooth, the interalveolar septum was selected by drawing a contour from the center of one root canal to another root canal by avoiding the roots and other structures. After scanning, 3-dimensional (3D) models were generated by CTVol (Skyscan), and the bone volume and density around the implants were analyzed using CTAn (Skyscan), which was also used to examine the μCT datasets for new bone growth. The collective sum of all ROI layers over a continuous set of cross-sectional image slices represented the volume of interest in the regenerated bone. Furthermore, new bone around the hole and bone mineral density (BMD) were calculated by phantom and Hounsfield units (HU) (low phantom [0.25] 1157.7907 HU and high phantom in μCT HU [0.75] 3233.3492 HU). Binary thresholds (gray-scale index, implant area: 160 mm × 255 mm; new bone area: 100 mm × 143 mm; and total bone area: 70 mm × 120 mm) were used to create the 3D images.

Histology and immunohistochemical staining

The mandibles were isolated and fixed in 10% neutral-buffered formalin solution. After fixation, the tissues were decalcified in 15% EDTA and 0.1 M Tris (pH 7.0). After decalcification, the implant was removed. The tissues were dehydrated with different percentage of alcohol, cleared in xylene, and embedded in paraffin. Tissue sections of 8 μm were mounted on glass slides and stained with hematoxylin and eosin (H&E) and immunohistochemical (IHC) stains. IHC staining was performed to detect the expression of IGFBP-3, BMP-2, BMP-7, osteoprotegerin (OPG), receptor activator of nuclear factor-κB ligand (RANKL), and receptor for advanced glycation end products (RAGE) using an immunohistochemistry accessory kit (Bethyl Laboratories, Montgomery, TX, USA). The primary antibodies were used at 1:200 dilutions according to the protocol. The slides were visualized microscopically (Carl Zeiss, Ostalbkreis, Germany). The levels of antibody expression were measured with ImageJ (National Institutes of Health, Bethesda, MD, USA) software.

Statistical analysis

All results were analyzed independently. All values are presented as the mean±standard deviation of 3 independent experiments. Statistical significance was assessed by the unpaired *t*-test. *P* values <0.05 were considered to indicate statistical significance. This *in vivo* study was conducted in groups containing 6 rats each.

https://doi.org/10.5051/jpis.2101200060

RESULTS

MGO impairs bone formation in MC3T3 E1 cells

MC3T3 E1 cells were treated with MGO (400 μM) in osteogenic medium for up to 15 days for the detection of osteogenic differentiation and mineralization. The cells treated with MGO demonstrated decreased Alizarin red staining in a time-dependent manner compared to the mock osteogenic medium (**Figure 1A**). Similarly, ALP activity was also significantly decreased by MGO treatment at 9, 12, and 15 days compared to the mock osteogenic medium (**Figure 1B**). The expression of osteogenic differentiation proteins (BMP-2, BMP-7, and OPG) was also decreased by MGO, whereas the expression of RANKL was increased by MGO treatment in a time-dependent manner (**Figure 1C**).

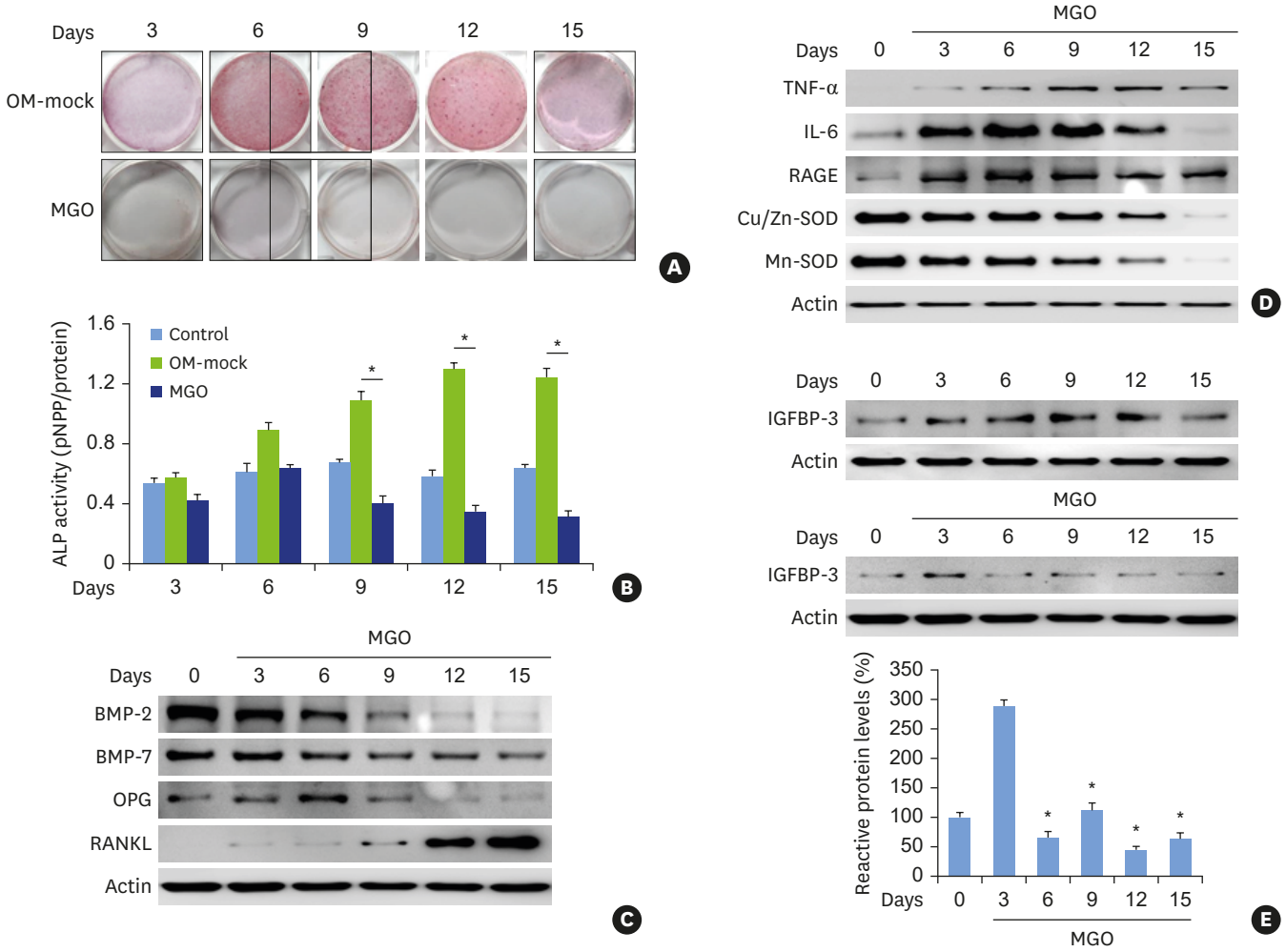

Figure 1. MGO impairs the function of bone formation in MC3T3 E1 cells. (A) Alizarin red staining after treatment of MC3T3 E1 cells with MGO for 3, 6, 9, 12, and 15 days. (B) Effects of MGO on ALP activity in MC3T3 E1 cells at 3, 6, 9, 12, and 15 days. MC3T3 E1 cells were treated with OM with 5 mM β-glycerol phosphate, 100 μM ascorbic acid, and 10 nM dexamethasone for the indicated times and ALP was measured. (C) Protein expression of BMP-2, BMP-7, RANKL, and OPG analyzed by western blots after treatment with MGO. (D) Effects of MGO on the expression of inflammatory proteins and anti-oxidant enzymes analyzed by western blots. (E) Expression of IGFBP-3 in MC3T3 E1 cells induced with or without MGO. Each value was reported as the mean±standard deviation of 3 experiments.
MGO: methylglyoxal, ALP: alkaline phosphatase, BMP: bone morphogenetic protein, OM: osteogenic medium, RANKL: receptor activator of nuclear factor-κB ligand, OPG: osteoprotegerin, IGFBP-3: insulin growth factor binding protein-3.
*P<0.05.

https://doi.org/10.5051/jpis.2101200060

MGO changes the expression of inflammatory, anti-oxidant, and IGFBP-3 proteins

Inflammation-related molecules (tumor necrosis factor-alpha [TNF-α], interleukin [IL]-6, and RAGE) were detected after the treatment of MC3T3 E1 cells with MGO. The cells demonstrated an increased expression of these molecules relative to controls (**Figure 1D**). Further, anti-oxidant activity was also evaluated by analyzing anti-oxidant molecules (Cu/Zn-superoxide dismutase [SOD] and Mn-SOD). These SOD enzymes were reduced in cells treated with MGO (**Figure 1D**). Similarly, the expression of IGFBP-3 protein also decreased after treatment with MGO (**Figure 1E**).

IGFBP-3 increases osteogenic differentiation and mineralization in MGO-treated MC3T3 E1 cells

The effect of *IGFBP-3* in the response to MGO (400 μM) was examined in MC3T3-E1 cells after treatment with the conjugated Ch-GNP/*IGFBP-3* complexes. Ch-GNP/*LacZ* complexes were used as the Ch-GNP control vector. The cells treated with Ch-GNPs/*LacZ* and MGO demonstrated decreased Alizarin red staining in a time-dependent manner. In contrast, the Ch-GNP/*IGFBP-3*-treated cells showed increased Alizarin red staining at 3, 9, and 15 days compared to the control Ch-GNP/*LacZ* cells, even when the cells were induced with MGO (**Figure 2A**). Correspondingly, ALP activity was also significantly increased by the Ch-GNP/

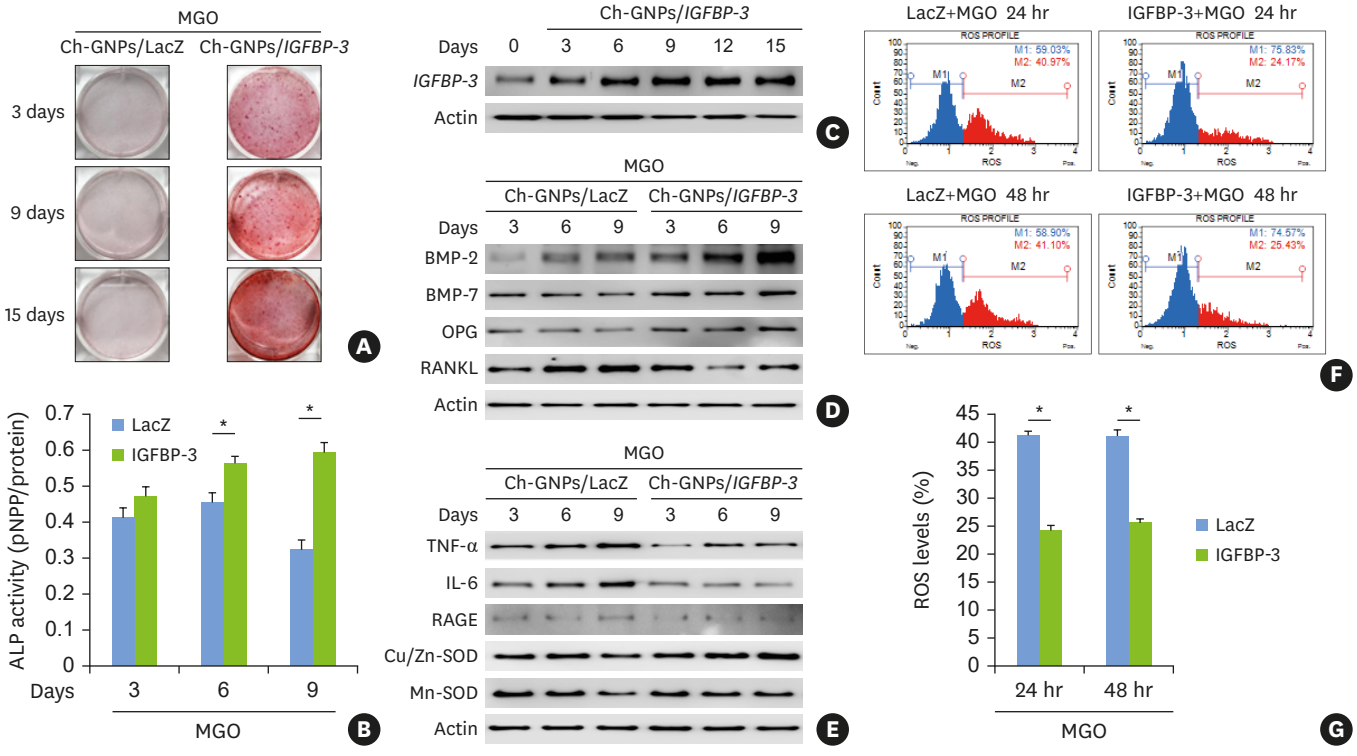

Figure 2. IGFBP-3 increased bone formation in MGO-treated MC3T3 E1 cells. (A) Analysis of osteogenic differentiation in response to Ch-GNPs/*IGFBP-3* in MC3T3 E1 cells induced with MGO and measurement of calcium deposition for matrix mineralization by Alizarin red staining. (B) Measurement of ALP activity by Ch-GNPs/*IGFBP-3* in MC-3T3 E1 cells induced with MGO. (C) Analysis of protein expression of *IGFBP-3* by western blots in MC3T3 E1 cells after treatment with Ch-GNPs/*IGFBP-3* and induction with MGO. (D) Expression of osteogenic-related proteins (BMP-2, BMP-7, and OPG) and an osteoclastic protein (RANKL). (E) Expression of inflammatory (TNF-α, IL-6, and RAGE) and anti-oxidant proteins. (F) Measurement of ROS formation by the Muse oxidative stress assay. (G) Graphical representation of ROS formation. Each value was reported as the mean±standard deviation of 3 experiments.
IGFBP-3: insulin growth factor binding protein-3, MGO: methylglyoxal, Ch-GNP: chitosan gold nanoparticle, MGO: methylglyoxal, BMP: bone morphogenetic protein, OPG: osteoprotegerin, RANKL: receptor activator of nuclear factor-κB ligand, TNF: tumor necrosis factor, IL: interleukin, RAGE: receptor for advanced glycation end products, ROS: reactive oxygen species.
*P<0.05.

https://doi.org/10.5051/jpis.2101200060

IGFBP-3 complexes at 6 and 9 days compared to Ch-GNPs/*LacZ* (**Figure 2B**). The expression of IGFBP-3 protein significantly increased up to 15 days after the cells were treated with conjugated Ch-GNPs/*IGFBP-3* (**Figure 2C**). MC3T3 E1 cells treated with the conjugated Ch-GNP/*IGFBP-3* complexes demonstrated higher expression levels of BMP-2, BMP-7, and OPG than the Ch-GNP/*LacZ* cells, even though the cells were induced with MGO. RANKL expression was decreased by Ch-GNPs/*IGFBP-3* treatment (**Figure 2D**).

IGFBP-3 activates anti-inflammatory and anti-oxidant expression in MGO-induced MC3T3 E1 cells

MGO-induced Ch-GNPs/*LacZ* cells demonstrated increased expressions of TNF-α, IL-6, and RAGE at the indicated times (**Figure 2E**). High expression of the anti-oxidant molecules Cu/Zn-SOD and Mn-SOD was seen in IGFBP-3-overexpressing MC3T3 E1 cells, even though the cells were induced with MGO (**Figure 2E**). The levels of ROS were analyzed 24 and 48 hours after the cells were induced with MGO. The ROS levels were significantly reduced in Ch-GNP/*IGFBP-3* cells compared to the Ch-GNPs/*LacZ* cells in a time-dependent manner (**Figure 2F and G**).

MGO reduces femur and alveolar bone formation in MGO-administered rats

μCT analysis and H&E staining were performed after the administration of MGO to rats. μCT examination of the femur 3 and 6 weeks after MGO administration demonstrated lower femoral cortical BMD, trabecular BMD, trabecular bone volume/total volume (BV/TV), trabecular number, trabecular thickness, and higher values for the femoral trabecular space compared to the controls (**Figure 3A**). However, μCT examination of the alveolar bone showed lower BMD and BV/TV in the MGO-administered group than in the control group (without MGO administered) at only 6 weeks (**Figure 3B**). The H&E staining results also confirmed a higher level of bone loss in the MGO-administered group at 3 and 6 weeks (**Figure 3C**).

IGFBP-3 restores mandibular bone deterioration in MGO-administered rats

To examine the role of IGFBP-3 in the osseointegration of dental implants in the MGO-administered rat model, the first molar of the rat mandibles was extracted and the recovery of bone deterioration was checked 3 and 6 weeks after MGO administration (**Figure 4A**). Bone formation by Ch-GNPs/*IGFBP-3* near the implant sites was higher than that of Ch-GNPs/*LacZ* in a time-dependent manner (**Figure 4B**). The 3D μCT images showed comparatively increased new bone formation, BMD, and BV in the Ch-GNP/*IGFBP-3* group (**Figure 4C**). Furthermore, H&E staining also confirmed the recovery of bone deterioration in response to Ch-GNP/*IGFBP-3*-coated implants in MGO-administered rat mandibles compared to the Ch-GNP/*LacZ* group at 3 and 6 weeks (**Figure 4D**).

Ch-GNP/*IGFBP-3*-coated implants decrease inflammatory molecules and increase osteogenic differentiation molecules in MGO-administered rats

IHC analysis demonstrated that the expression of IGFBP-3 increased at 3 and 6 weeks in the Ch-GNP/*IGFBP-3*-coated implant group (**Figure 5A**). These results indicated that the Ch-GNPs carried the reporter gene to the implantation site. Levels of inflammation-related molecules (TNF-α, IL-6, and RAGE) were increased in the Ch-GNP/*LacZ*-coated implant group 3 and 6 weeks after the administration of MGO, whereas levels of these molecules decreased in the Ch-GNP/*IGFBP-3*-coated implant group even with MGO administration (**Figure 5A and B**).

The expression of osteogenic differentiation molecules near the implant site was identified by IHC. The expression of BMP-2, BMP-7, and OPG was higher in the MGO-administered Ch-GNP/*IGFBP-3*-coated implant group than in the Ch-GNP/*LacZ*-coated implant group at 3 and 6

https://doi.org/10.5051/jpis.2101200060

JPIS
Journal of Periodontal & Implant Science

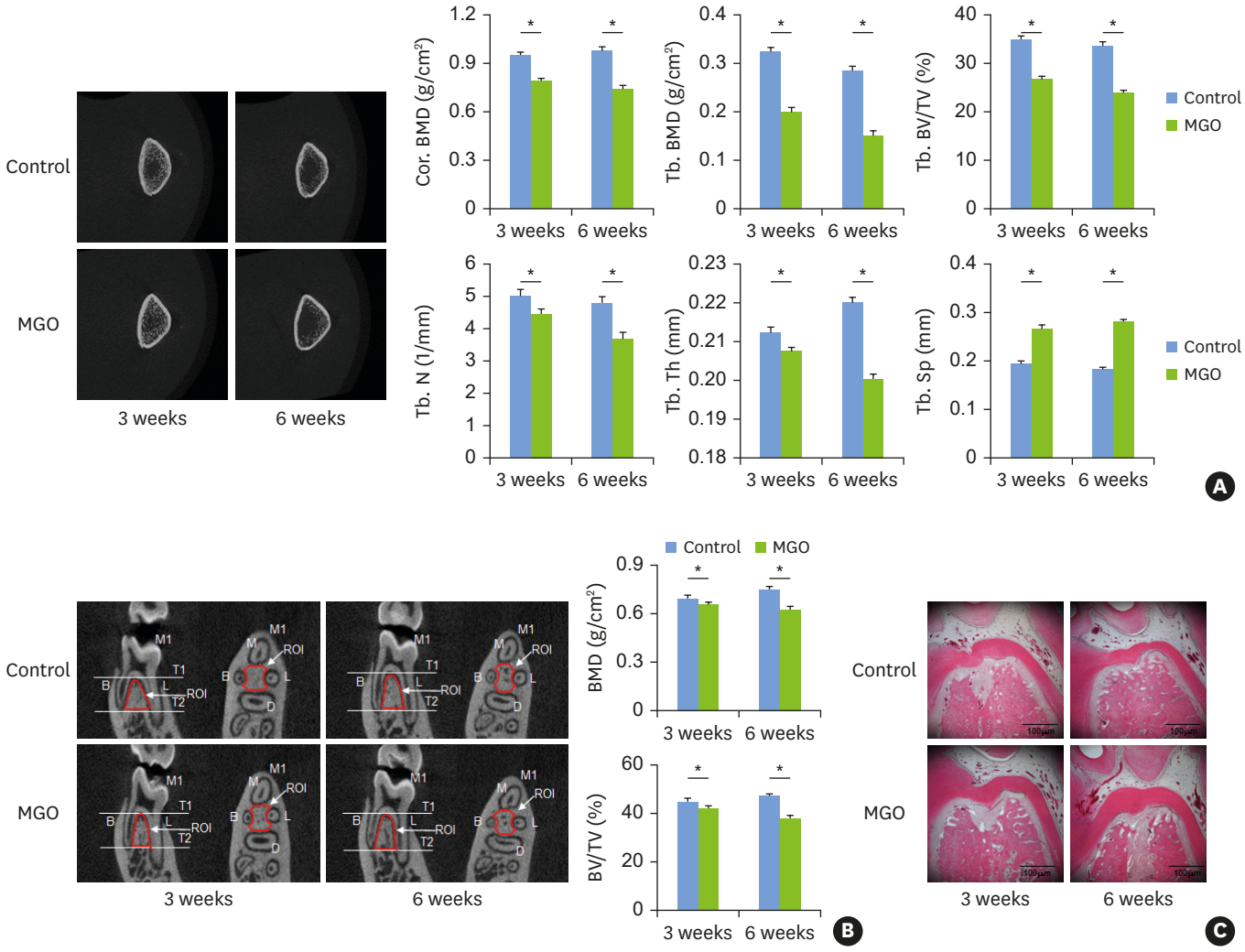

Figure 3. MGO impairs femur and alveolar bone formation in MGO-administered rats. (A) μCT (2-dimensional) imaging of rat femur after the administration of MGO (75 mg/kg) for 3 and 6 weeks. Analysis of femoral cortical BMD, trabecular BMD, BV/TV, trabecular number, thickness, and space. (B) Detection of changes in rat alveolar bone by 2-dimensonal μCT after the administration of MGO and analysis of mandible BMD and BV/TV. M1: the mandibular first molar; M: mesial root; B: buccal root; D: distal root; L: lingual root; and T1 and T2: the 2 parallel horizontal planes passing through the alveolar ridge and the apex of the buccal muscle separately. (C) H&E staining of rat mandible with or without the administration of MGO. Data are expressed as mean±SEM at 3 and 6 weeks (n=6). MGO: methylglyoxal, μCT, micro-computed tomography, BMD: bone mineral density, BV: bone volume, TV: total volume, H&E: hematoxylin and eosin, SEM: standard error of the mean.
*P<0.05.

weeks (**Figure 6A and B**). The osteoclast-related molecule RANKL was more highly expressed in the MGO-administered Ch-GNPs/*LacZ*-coated implant group than in the Ch-GNPs/*IGFBP-3*-coated implant group in a time-dependent manner (**Figure 6B**).

DISCUSSION

MGO has been found to decrease bone mineral density in an animal model [16]. MGO and MGO-derived AGEs are normally associated with the development of DM and its complications [36]. DM may decrease bone density and increase the risk of chronic inflammation, which advances to bone-related pathology such as osteoporosis, which is

https://doi.org/10.5051/jpis.2101200060

JPIS
Journal of Periodontal & Implant Science

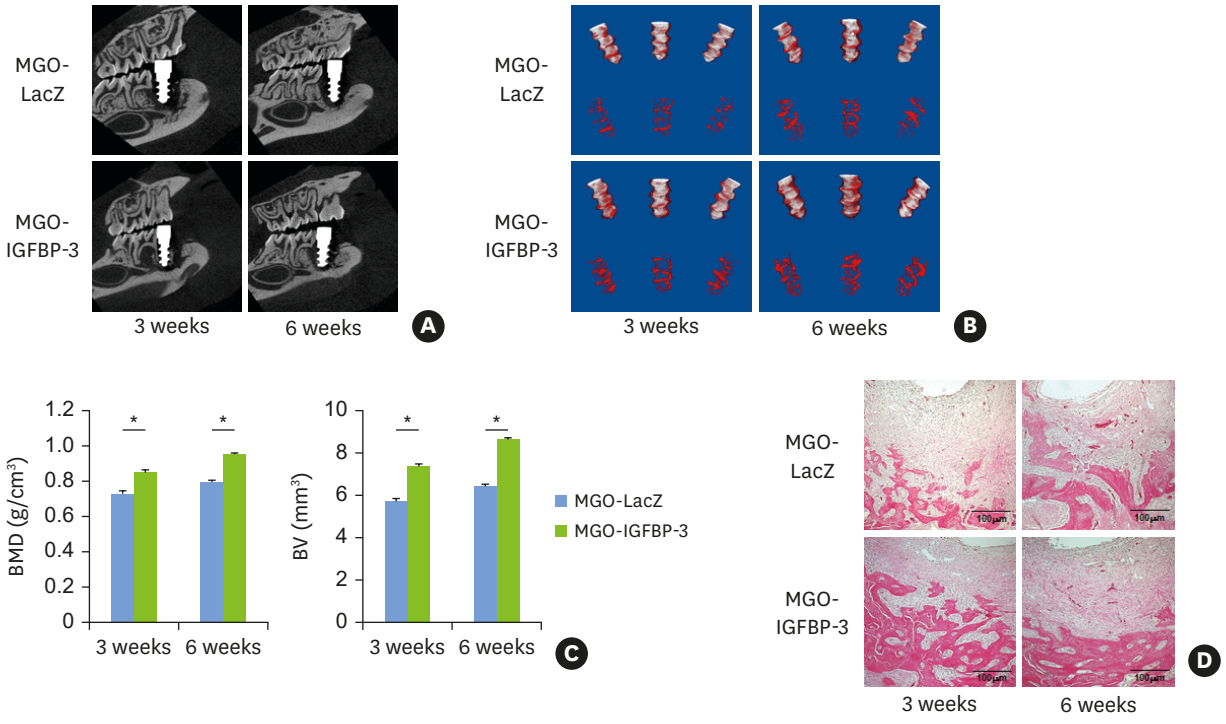

Figure 4. *IGFBP-3* restores MGO-induced bone deterioration in MGO-administered rats. (A) Two-dimensional μCT analysis of Ch-GNP/*LacZ*- and Ch-GNs/*IGFBP-3*-coated implants 3 and 6 weeks after the administration of MGO. (B) Three-dimensional μCT analysis of Ch-GNP/*LacZ*- and Ch-GNPs/*IGFBP-3*-coated implants. (C) Analysis of BMD and BV/TV. (D) H&E staining of the mandible around the implant surface 3 and 6 weeks after implantation. Data are expressed as mean ± SEM at 3 and 6 weeks (n=6).
IGFBP-3: insulin growth factor binding protein-3, MGO: methylglyoxal, μCT, micro-computed tomography, Ch-GNP: chitosan gold nanoparticle, BMD: bone mineral density, BV: bone volume, TV: total volume, H&E: hematoxylin and eosin, SEM: standard error of the mean.
*$P<0.05$.

one of the major complications of DM [3]. Furthermore, ROS accumulate in DM and impair the biological performance of osteoblastic cells on Ti surfaces [37]. Delivery of the *IGFBP-3* gene upregulated osteogenesis, downregulated osteoclastogenesis, and enhanced bone remodeling around the Ti surfaces of dental implants [27]. This study demonstrated the role of Ch-GNPs/*IGFBP-3* in MGO-induced bone deterioration and inflammation in MGO-treated MC3T3 E1 cells and a Sprague-Dawley rat animal model.

The increased expression of IGFBP-3 by Ch-GNP/*IGFBP-3* indicated that Ch-GNPs easily carried *IGFBP-3* plasmid DNA to the cells and alveolar bone in the targeted area. Alizarin red staining was used to detect mineralization nodules during bone formation in the MC3T3 E1 cells. Similarly, ALP activity is an early differentiation marker of osteoblastic mineralization and maturation [38]. In this study, MGO reduced Alizarin red staining and ALP activity in MC3T3 E1 cells, indicating that MGO affected osteoblastic mineralization and bone matrix maturation. However, the increased Alizarin red staining and ALP activity in MGO-induced MC3T3 E1 cells pretreated with Ch-GNPs/*IGFBP-3* suggested that *IGFBP-3* enhanced osteoblastic mineralization.

The present study demonstrated that MGO decreased osteogenic molecules (BMP-2, BMP-7, and OPG) and increased the expression of RANKL in MC3T3 E1 cells. BMP is involved in bone formation by osteoblast differentiation [39]. RANKL regulates bone destruction by stimulating osteoclastogenesis [40]. OPG promotes osteoblastogenesis by inhibiting osteoclastogenesis with minimization of RANKL [41]. In this study, the decreased

https://doi.org/10.5051/jpis.2101200060

JPIS
Journal of Periodontal & Implant Science

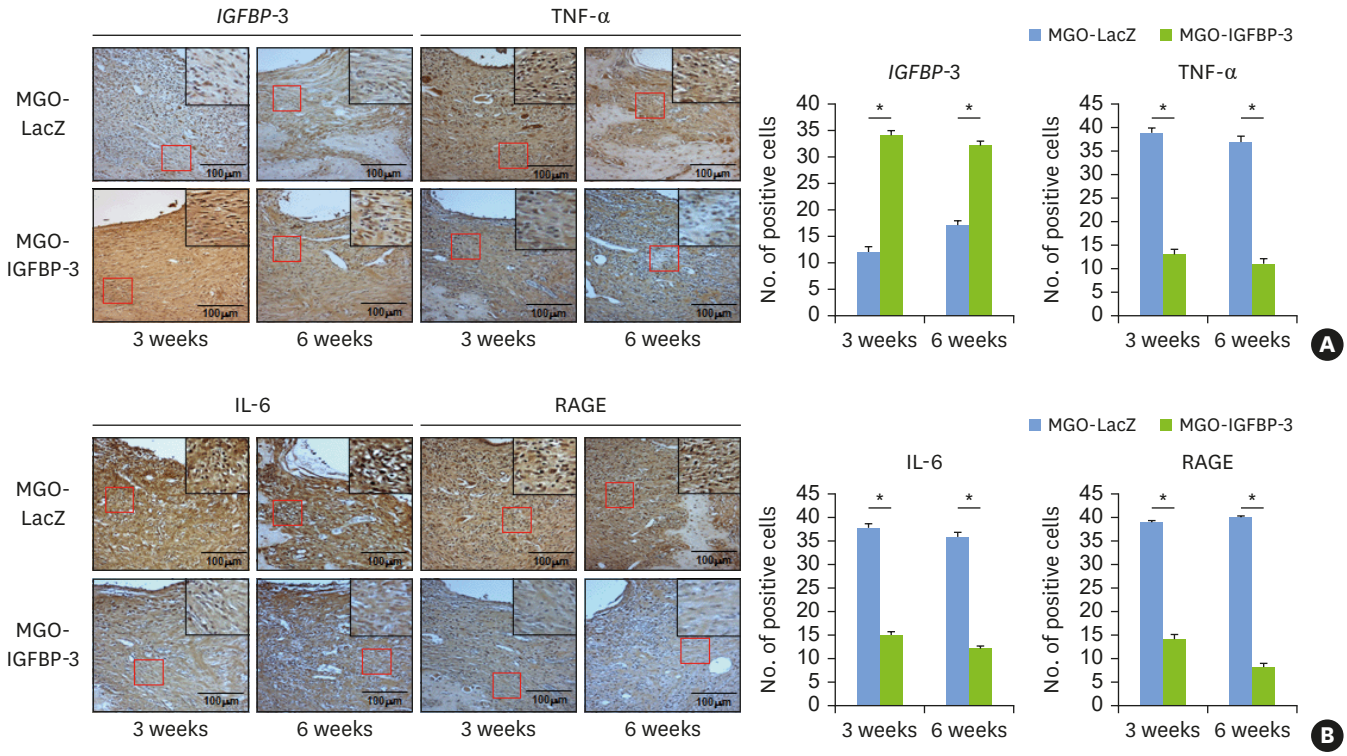

Figure 5. Ch-GNP/*IGFBP-3*-coated implants inhibit inflammatory proteins in MGO-administered rats. (A, B) Analysis of *IGFBP-3*, TNF-α, IL-6, and RAGE by IHC staining after 3 and 6 weeks. The intensity specific for the brown color correlates with the protein level.
Ch-GNP: chitosan gold nanoparticle, IGFBP-3: insulin growth factor binding protein-3, MGO: methylglyoxal, TNF: tumor necrosis factor, IL: interleukin, RAGE: receptor for advanced glycation end products, IHC: immunohistochemistry.
*$P<0.05$.

expression of BMP and OPG, and increased expression of RANKL by MGO indicated that MGO interfered with osteoblast differentiation and bone formation, and enhanced osteoclastogenesis and bone resorption. Nevertheless, the recovered expression of BMP-2, BMP-7, and OPG, and downregulation of RANKL by *IGFBP-3* in MGO-induced MC3T3 E1 cells indicated that *IGFBP-3* recovered osteogenesis and bone formation by inhibiting osteoclastogenesis in MGO-induced bone cell deterioration.

MGO can activate inflammatory molecules with excess formation of pro-inflammatory cytokines through oxidative stress [42]. MGO produces high amounts of ROS, which is one of the major causes of oxidative stress and is responsible for DM-related impairments in cognitive function [12,13]. RAGE evokes oxidative stress with increases in ROS formation that stimulate the production of pro-inflammatory cytokines (TNF-α and IL-6) [43]. The present study also demonstrated increased levels of ROS, RAGE, TNF-α, and IL-6, and decreased expression of antioxidant enzymes (Cu/Zn-SOD and Mn-SOD) after the treatment of MC3T3 E1 cells with MGO, and these results were associated with the effects of MGO. In addition, IGFBP-3 effectively reduced oxidative stress as well as inflammatory molecules, even with MGO treatment. Thus, these results suggest that IGFBP-3 may be able to minimize the oxidative stress and inflammation produced by MGO and influence the formation of bone-related proteins, which considerably promote osteogenesis and inhibit bone resorption.

A distinct decrease in bone mineral density and bone volume appeared at the femur site and mandible in MGO-administered rats compared to the control group in this study. Moreover,

https://doi.org/10.5051/jpis.2101200060

JPIS
Journal of Periodontal & Implant Science

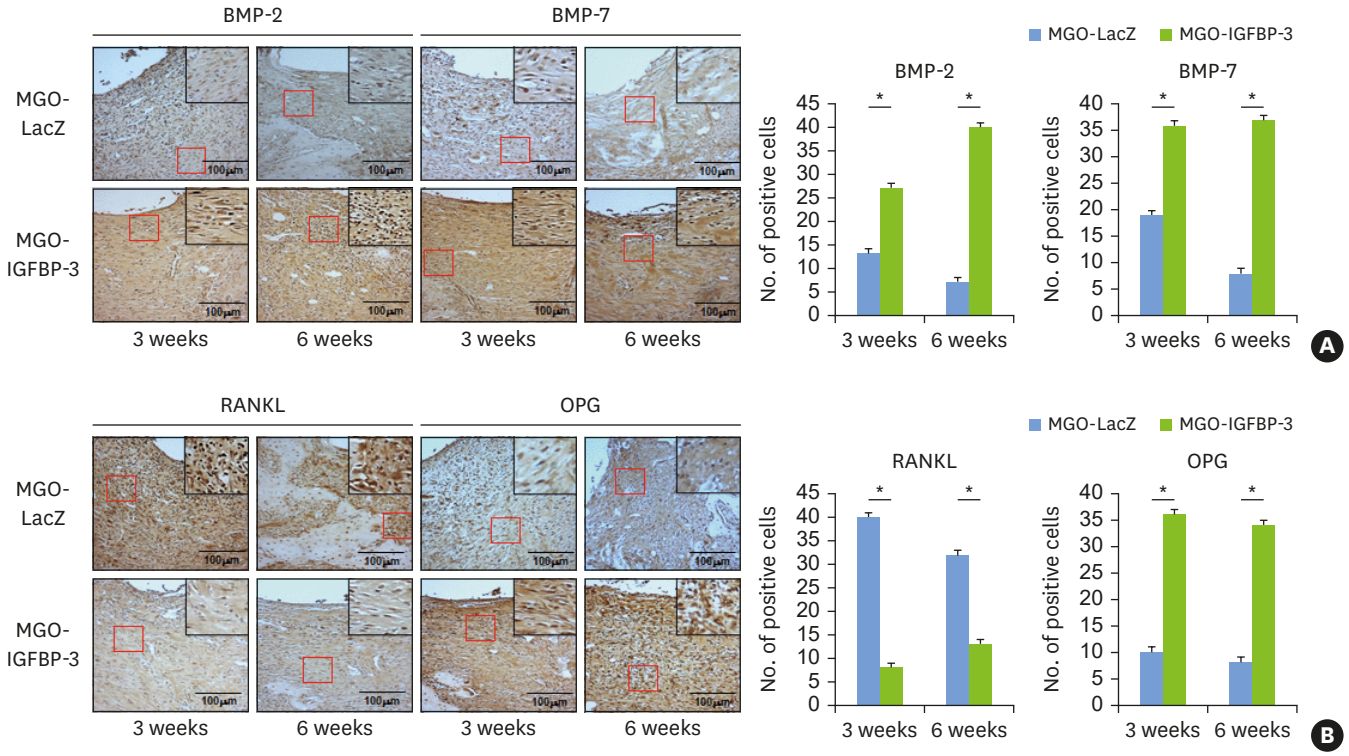

Figure 6. Ch-GNP/*IGFBP-3*-coated implants increase osteogenic differentiation in MGO-administered rats. (A, B) IHC staining of BMP-2, BMP-7, OPG, and RANKL for the detection of osteoblast differentiation. The intensity specific for the brown color correlates with the protein level.
Ch-GNP: chitosan gold nanoparticle, IGFBP-3: insulin growth factor binding protein-3, MGO: methylglyoxal, IHC: immunohistochemistry, BMP: bone morphogenetic protein, OPG: osteoprotegerin, RANKL: receptor activator of nuclear factor-κB ligand.
*$P<0.05$.

MGO affected various histological phenomena, such as femoral trabeculae and minimal new bone growth in the mandible relative to normal rats. Thus, these results suggested that MGO induced oxidative stress and an inflammatory reaction, and hindered bone formation.

The role of IGFBP-3 in osteogenic differentiation and bone formation has been well studied [27,44,45]. Our previous study successfully demonstrated that Ch-GNP/*IGFBP-3*-coated dental implants promoted osseointegration and bone formation in the implant insertion area [27]. We hypothesized that delivery of the *IGFBP-3* gene may overcome inflammation and support regional bone regeneration, thereby overcoming MGO interference in the MGO-administered rat model. In this study, when *IGFBP-3* was applied to implants in the rat model induced with MGO, increased bone mineral density, bone volume, and new bone formation were seen, even under MGO stress. In IHC staining, the restoration of bone formation-related molecules (BMP-2, BMP-7, and OPG) and alleviation of inflammatory protein expression (TNF-α, IL-6, RAGE, and RANKL) were dependent upon *IGFBP-3* expression. These results suggested that the application of *IGFBP-3* seemed to improve MGO-induced stress at the regional sites of the dental implants and supported dental implant osseointegration and minimized bone resorption.

In conclusion, MGO-induced oxidative stress and inflammation could be minimized by the application of Ch-GNPs/*IGFBP-3* to titanium dental implants, which supported bone formation near the implantation site. In summary, the overall results of this study, within some limitations, showed that the generation of regional *IGFBP-3* gene expression by dental implants may provide an appropriate therapeutic approach for osseointegration in MGO-

https://doi.org/10.5051/jpis.2101200060

induced stress and DM. To develop a treatment modality that can be applied to patients with diabetes who have increased MGO levels, more detailed research is needed in the future.

REFERENCES

1. Arroyave F, Montaño D, Lizcano F. Diabetes mellitus is a chronic disease that can benefit from therapy with induced pluripotent stem cells. Int J Mol Sci 2020;21:8685.
PUBMED | CROSSREF
2. Kim JB, Jung MH, Cho JY, Park JW, Suh JY, Lee JM. The influence of type 2 diabetes mellitus on the expression of inflammatory mediators and tissue inhibitor of metalloproteinases-2 in human chronic periodontitis. J Periodontal Implant Sci 2011;41:109-16.
PUBMED | CROSSREF
3. Jiao H, Xiao E, Graves DT. Diabetes and its effect on bone and fracture healing. Curr Osteoporos Rep 2015;13:327-35.
PUBMED | CROSSREF
4. Farr JN, Drake MT, Amin S, Melton LJ 3rd, McCready LK, Khosla S. *In vivo* assessment of bone quality in postmenopausal women with type 2 diabetes. J Bone Miner Res 2014;29:787-95.
PUBMED | CROSSREF
5. Chrcanovic BR, Albrektsson T, Wennerberg A. Diabetes and oral implant failure: a systematic review. J Dent Res 2014;93:859-67.
PUBMED | CROSSREF
6. Daubert DM, Weinstein BF, Bordin S, Leroux BG, Flemming TF. Prevalence and predictive factors for peri-implant disease and implant failure: a cross-sectional analysis. J Periodontol 2015;86:337-47.
PUBMED | CROSSREF
7. Michaeli E, Weinberg I, Nahlieli O. Dental implants in the diabetic patient: systemic and rehabilitative considerations. Quintessence Int 2009;40:639-45.
PUBMED
8. Oates TW, Huynh-Ba G, Vargas A, Alexander P, Feine J. A critical review of diabetes, glycemic control, and dental implant therapy. Clin Oral Implants Res 2013;24:117-27.
PUBMED | CROSSREF
9. Brownlee M, Cerami A, Vlassara H. Advanced glycosylation end products in tissue and the biochemical basis of diabetic complications. N Engl J Med 1988;318:1315-21.
PUBMED | CROSSREF
10. Bourajjaj M, Stehouwer CD, van Hinsbergh VW, Schalkwijk CG. Role of methylglyoxal adducts in the development of vascular complications in diabetes mellitus. Biochem Soc Trans 2003;31:1400-2.
PUBMED | CROSSREF
11. Kim KM, Kim YS, Jung DH, Lee J, Kim JS. Increased glyoxalase I levels inhibit accumulation of oxidative stress and an advanced glycation end product in mouse mesangial cells cultured in high glucose. Exp Cell Res 2012;318:152-9.
PUBMED | CROSSREF
12. Messier C, Gagnon M. Glucose regulation and cognitive functions: relation to Alzheimer's disease and diabetes. Behav Brain Res 1996;75:1-11.
PUBMED | CROSSREF
13. Gerozissis K. Brain insulin: regulation, mechanisms of action and functions. Cell Mol Neurobiol 2003;23:1-25.
PUBMED | CROSSREF
14. Bouillon R. Diabetic bone disease. Calcif Tissue Int 1991;49:155-60.
PUBMED | CROSSREF
15. Chan WH, Wu HJ, Shiao NH. Apoptotic signaling in methylglyoxal-treated human osteoblasts involves oxidative stress, c-Jun N-terminal kinase, caspase-3, and p21-activated kinase 2. J Cell Biochem 2007;100:1056-69.
PUBMED | CROSSREF
16. Lee KM, Lee CY, Zhang G, Lyu A, Yue KK. Methylglyoxal activates osteoclasts through JNK pathway leading to osteoporosis. Chem Biol Interact 2019;308:147-54.
PUBMED | CROSSREF
17. Aikawa T, Matsubara H, Ugaji S, Shirakawa J, Nagai R, Munesue S, et al. Contribution of methylglyoxal to delayed healing of bone injury in diabetes. Mol Med Rep 2017;16:403-9.
PUBMED | CROSSREF

18. Jemat A, Ghazali MJ, Razali M, Otsuka Y. Surface modifications and their effects on titanium dental implants. BioMed Res Int 2015;2015:791725.
PUBMED | CROSSREF

19. Moraschini V, Poubel LA, Ferreira VF, Barboza ES. Evaluation of survival and success rates of dental implants reported in longitudinal studies with a follow-up period of at least 10 years: a systematic review. Int J Oral Maxillofac Surg 2015;44:377-88.
PUBMED | CROSSREF

20. Chen S, Yang J, Wang H, Chao Y, Zhang C, Shen J, et al. Adenovirus encoding BMP-7 immobilized on titanium surface exhibits local delivery ability and regulates osteoblast differentiation *in vitro*. Arch Oral Biol 2013;58:1225-31.
PUBMED | CROSSREF

21. Wang Y, Huang L. Composite nanoparticles for gene delivery. Adv Genet 2014;88:111-37.
PUBMED | CROSSREF

22. Bhattarai G, Lee YH, Lee MH, Yi HK. Gene delivery of c-myb increases bone formation surrounding oral implants. J Dent Res 2013;92:840-5.
PUBMED | CROSSREF

23. Bhattarai G, Lee YH, Lee NH, Park IS, Lee MH, Yi HK. PPARγ delivered by Ch-GNPs onto titanium surfaces inhibits implant-induced inflammation and induces bone mineralization of MC-3T3E1 osteoblast-like cells. Clin Oral Implants Res 2013;24:1101-9.
PUBMED | CROSSREF

24. Lee YH, Kim JS, Kim JE, Lee MH, Jeon JG, Park IS, et al. Nanoparticle mediated PPARγ gene delivery on dental implants improves osseointegration via mitochondrial biogenesis in diabetes mellitus rat model. Nanomedicine (Lond) 2017;13:1821-32.
PUBMED | CROSSREF

25. Lieberman JR, Daluiski A, Einhorn TA. The role of growth factors in the repair of bone. Biology and clinical applications. J Bone Joint Surg Am 2002;84:1032-44.
PUBMED | CROSSREF

26. Firth SM, Baxter RC. Cellular actions of the insulin-like growth factor binding proteins. Endocr Rev 2002;23:824-54.
PUBMED | CROSSREF

27. Bhattarai G, Lee YH, Lee MH, Park IS, Yi HK. Insulin-like growth factor binding protein-3 affects osteogenic efficacy on dental implants in rat mandible. Mater Sci Eng C 2015;55:490-6.
PUBMED | CROSSREF

28. Kawai M, Rosen CJ. The insulin-like growth factor system in bone: basic and clinical implications. Endocrinol Metab Clin North Am 2012;41:323-33.
PUBMED | CROSSREF

29. Chard T. Insulin-like growth factors and their binding proteins in normal and abnormal human fetal growth. Growth Regul 1994;4:91-100.
PUBMED

30. Magnucki G, Schenk U, Ahrens S, Navarrete Santos A, Gernhardt CR, Schaller HG, et al. Expression of the IGF-1, IGFBP-3 and IGF-1 receptors in dental pulp stem cells and impacted third molars. J Oral Sci 2013;55:319-27.
PUBMED | CROSSREF

31. Galluzzi L, Vitale I, Abrams JM, Alnemri ES, Baehrecke EH, Blagosklonny MV, et al. Molecular definitions of cell death subroutines: recommendations of the Nomenclature Committee on Cell Death 2012. Cell Death Differ 2012;19:107-20.
PUBMED | CROSSREF

32. Johnson MA, Firth SM. IGFBP-3: a cell fate pivot in cancer and disease. Growth Horm IGF Res 2014;24:164-73.
PUBMED | CROSSREF

33. Kim JE, Takanche JS, Kim JS, Lee MH, Jeon JG, Park IS, et al. Phelligridin D-loaded oral nanotube titanium implant enhances osseointegration and prevents osteolysis in rat mandible. Artif Cells Nanomed Biotechnol 2018;46:397-407.
PUBMED | CROSSREF

34. Takanche JS, Kim JE, Kim JS, Lee MH, Jeon JG, Park IS, et al. Chitosan-gold nanoparticles mediated gene delivery of c-myb facilitates osseointegration of dental implants in ovariectomized rat. Artif Cells Nanomed Biotechnol 2018;46:S807-17.
PUBMED | CROSSREF

35. Berlanga J, Cibrian D, Guillén I, Freyre F, Alba JS, Lopez-Saura P, et al. Methylglyoxal administration induces diabetes-like microvascular changes and perturbs the healing process of cutaneous wounds. Clin Sci (Lond) 2005;109:83-95.
PUBMED | CROSSREF

36. Chilelli NC, Burlina S, Lapolla A. AGEs, rather than hyperglycemia, are responsible for microvascular complications in diabetes: a "glycoxidation-centric" point of view. Nutr Metab Cardiovasc Dis 2013;23:913-9.
PUBMED | CROSSREF

37. Feng YF, Wang L, Zhang Y, Li X, Ma ZS, Zou JW, et al. Effect of reactive oxygen species overproduction on osteogenesis of porous titanium implant in the present of diabetes mellitus. Biomaterials 2013;34:2234-43.
PUBMED | CROSSREF

38. Suh KS, Chon S, Choi EM. Bergenin increases osteogenic differentiation and prevents methylglyoxal-induced cytotoxicity in MC3T3-E1 osteoblasts. Cytotechnology 2018;70:215-24.
PUBMED | CROSSREF

39. Bessa PC, Casal M, Reis RL. Bone morphogenetic proteins in tissue engineering: the road from the laboratory to the clinic, part I (basic concepts). J Tissue Eng Regen Med 2008;2:1-13.
PUBMED | CROSSREF

40. Young PS, Tsimbouri PM, Gadegaard N, Meek RM, Dalby MJ. Osteoclastogenesis/osteoblastogenesis using human bone marrow-derived cocultures on nanotopographical polymer surfaces. Nanomedicine (Lond) 2015;10:949-57.
PUBMED | CROSSREF

41. Teitelbaum SL. Osteoclasts, integrins, and osteoporosis. J Bone Miner Metab 2000;18:344-9.
PUBMED | CROSSREF

42. Shanmugam N, Kim YS, Lanting L, Natarajan R. Regulation of cyclooxygenase-2 expression in monocytes by ligation of the receptor for advanced glycation end products. J Biol Chem 2003;278:34834-44.
PUBMED | CROSSREF

43. Bansal S, Siddarth M, Chawla D, Banerjee BD, Madhu SV, Tripathi AK. Advanced glycation end products enhance reactive oxygen and nitrogen species generation in neutrophils *in vitro*. Mol Cell Biochem 2012;361:289-96.
PUBMED | CROSSREF

44. Evans DS, Cailotto F, Parimi N, Valdes AM, Castaño-Betancourt MC, Liu Y, et al. Genome-wide association and functional studies identify a role for IGFBP3 in hip osteoarthritis. Ann Rheum Dis 2015;74:1861-7.
PUBMED | CROSSREF

45. Deng M, Luo K, Hou T, Luo F, Xie Z, Zhang Z, et al. IGFBP3 deposited in the human umbilical cord mesenchymal stem cell-secreted extracellular matrix promotes bone formation. J Cell Physiol 2018;233:5792-804.
PUBMED | CROSSREF

https://doi.org/10.5051/jpis.2101200060